On the Effect of Multi-Packet Reception on Redundant Gateways in LoRAWANs

Minming Ni*, Mehdi Jafarizadeh†, Rong Zheng†
*State Key Lab. of Rail Traffic Control and Safety, Beijing Jiaotong University, Beijing, China
†Department of Computing and Software, McMaster University, Hamilton, ON, Canada

***Abstract*—In this paper, the impact of redundant packet reception at multiple gateways on data reliability is studied under the LoRaWAN architecture. Given a successful transmission could be the result of either a first attempt after a data packet's generation, or a retry after several transmission failures, the Average Successful Transmission Probability (ASTP) is introduced to qualify LoRaWAN's reliability performance. To calculate the probability of a successful reception without retransmission, we consider all the possible causes for a packet collision. The number of potential interferers, which is vital for the collision analyses and directly determined by the relative locations of the relevant multiple gateways, is determined by geometric arguments. Similarly, the probability for achieving a successful retransmission is also obtained. Finally, ASTP is rigorously modeled as a function of end device density, gateway density, and traffic intensity. The analytical results have been verified by extensive simulation experiments. We believe that the analytical model can provide useful insights into the scalability of LoRaWANs and provide guidelines for their deployments.**

I. Introduction

The proliferation of the Internet of Things (IoTs) drives the demand for enabling reliable wireless communications with low-bandwidth connectivity. Among all the existing technologies, LoRa (Long Range), which relies on the Chirp Spread Spectrum (CSS) modulation, has attracted much attention due to its ability to support very-long-range transmissions (more than 10 km in rural areas) with low power consumption. With LoRa as the physical layer, LoRa Alliance™ standardized a medium access control protocol LoRaWAN [1], which is deployed in a star-of-stars topology shown in Fig. 1. In LoRaWAN, the data packets generated by end devices are wirelessly transmitted to gateways and further forwarded to the network servers via standard IP connections. Moreover, each end device is not assigned to a specific gateway, which means higher network scalability and transmission reliability, as the data packets can be received by any gateway in range.

Since the release of LoRaWAN specification, several papers have evaluated the radio performance of LoRa regarding the spreading factor, code rate, and transmission power [2], [3], or with consideration of external factors like Doppler effect [4]. Complementary to LoRa radio analysis, some studies assessed the scalability of the LoRaWAN protocol using simulations [5] or experiments [6]. Since LoRaWAN is an ALOHA-based MAC protocol and with no carrier sensing before transmission, the few papers that analytically studied the performance of LoRaWAN incorporated known results of deterministic ALOHA [7], [8]. However, to the best of our knowledge, the effect of redundant packet receptions in the multiple gateways, which can play an important role in the reliability of LoRaWAN, was never investigated analytically. In other words, existing analytical models cannot fully characterize the reliability of LoRaWAN especially for the scenarios, where the gateways are densely deployed and each IoT device is covered by more than one of them. The lack of an accurate and efficient analytical model hampers a comprehensive understanding of how the design parameters affect the overall network performance.

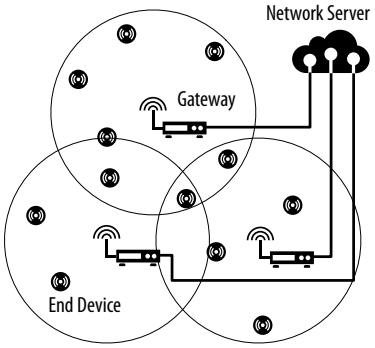

Fig. 1. Network Architecture of LoRaWAN

In this paper, we analyze the impact of redundant gateway deployment on transmission reliability using probabilistic and stochastic geometric techniques. Since a transmission can be either a first attempt after a data packet's generation or a retry after several transmission failures, exact characterization of the *Average Successful Transmission Probability* (ASTP) in presence of multiple gateway reception is non-trivial. Specifically, the probability of a data packet to be successfully received without retransmission can be divided into three parts as the probabilities that 1) no collision happens between the tagged data packet transmission and any other data packets, 2) no collision happens between the tagged transmission and other data packets' acknowledgments (ACKs), and 3) the ACK for the tagged data packet can be successfully received. To calculate the three probabilities, the number of possible collisions/interferers, which is determined by gateways' relative positions, is obtained via stochastic geometrical arguments. Similarly, the success probability for a retransmission can also be derived. Finally, the ASTP for an IoT device covered by multiple gateways simultaneously can be acquired as a function of gateway density, IoT device density, and traffic generation intensity. To the best of our knowledge, this is the first work that analyzes LoRaWAN performance with redundant gateways. The model can provide insights to the

978-1-5386-8088-9/19/$31.00 ©2019 IEEE

scalability and deployment configurations of LoRaWANs.

The remaining part of this paper is organized as follow. In the next section, the problem is formulated and the system model is illustrated. In Section III, the successful transmission probability with multiple gateway coverage is derived, while the related geometrical calculations are provided in Section IV. The analytic results are validated by simulations in Section V, and Section VI concludes this paper.

II. System Model

In this paper, we aim to study packet transmission reliability under the typical two-tier network architecture of LoRaWAN, when the tagged transmitting end device is covered by n gateways at the same time. To analyze the outcome of concurrent wireless transmissions, the well-known *Protocol Interference Model* [9] is adopted in this paper. Analyses using more complex physical interference model will be conducted as part of our future work. According to the protocol interference model, a successful transmission occurs when a node falls inside the transmission range of its intended transmitter and falls outside the interference ranges of other unintended transmitters. More specifically for multiple gateways, a data packet can be finally collected by a network server as long as *any* of the n gateways can receive the packet correctly. Therefore, packet collisions or co-channel interference can be partially mitigated by the redundant packet receptions at gateways. However, since the interference range is always larger than the transmission range, the multiple gateways' interference regions are partially overlapped with each other. In other words, the successful reception probabilities at each gateway are correlated.

For tractability of the analysis, we assume that all the end devices are uniformly distributed with density ρ (nodes per unit area). Data packets with the identical size L_{D} are generated at each device independently according to a Poisson process with density λ (packets per second). Once a packet is ready, it is modulated with CSS mechanism, and broadcast on one of the C main channels with data rate R_m, where $m \in [0, M]$ is the data rate code defined by the LoRaWAN specifications. Note that the data rate is determined by the selected spreading factor and channel bandwidth. Therefore, a collision only occurs when two packets are transmitted in the same channel at the same data rate, and their transmitting durations overlap with each other. The selection of data rate is application specific, and in our analysis, we assume data rate R_m is selected with probability P_m^{R}, which is known to the system. After the uplink transmission, the end device sets up two reception windows to receive the ACK for the correct packet reception as shown in Fig. 2. The first window starts on the previously used main channel at time $T_1 + T_m^{\mathsf{D}}$, where $T_m^{\mathsf{D}} = L_{\mathsf{D}}/R_m$ is the completion time of the uplink transmission with data rate R_m, and the second one is one second later on a specific downlink channel. If no ACK is received till the ACK_TIMEOUT waiting duration $T_{\mathsf{A\text{-}Out}}$ is over, the end device will re-select a main channel and initialize a retransmission with a random offset time $t_{\mathsf{Re}} - \tau$, where $\tau = T_m^{\mathsf{D}} + T_{\mathsf{A\text{-}Out}}$, drawn from $[1, 1 + W]$ seconds, and W is the pre-defined maximum backoff time duration. The number of total retransmissions is limited by N.

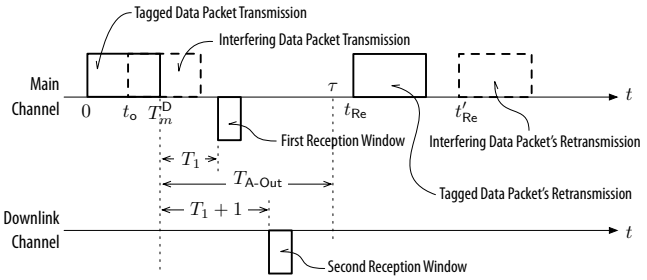

Fig. 2. Timeline for Data Transmission, Reception Windows, and Retransmission

TABLE I
Mathematical Notations

G_i	Gateway i	I_i	Interference Region of G_i
ρ	End Device Density	λ	Traffic Intensity
L_{D}	Data Packet Size	L_{A}	ACK Packet Size
C	Number of Main Channels	N	Max Retrans. Time
R_m	Data Rate for Code m	P_m^{R}	Prob. for R_m
d_{G}	Min Inter-Gateway Distance	P_n	Ave. Succ. Trans. Prob.
P_{1st}	Prob. for Picking Up a First Transmission		
P_n^{1st}	Prob. for Successful Trans at First Attempt		
$P_{m,n}^{\mathsf{DATA}}$	Prob. for Zero Coll. on Data Packet Trans., Given n, R_m		
$P_{m,n}^{\mathsf{ACK}}$	Prob. for Zero Coll. on ACK Packet Trans., Given n, R_m		
$P_{m,n}^{\mathsf{D\text{-}D}}$	Prob. for Zero Coll. Between Data Packets, Given n, R_m		
$P_{m,n}^{\mathsf{D\text{-}A}}$	Prob. for Zero Coll. Between Data and ACK, Given n, R_m		
$P_{m,n}^{\mathsf{D\text{-}Re}}$	Prob. for Zero Coll. on Data Packet Retrans., Given n, R_m		

In the analysis, we assume all the gateways are deployed on regular grids, and the shortest distance between two gateways is d_{G}. Based on different application categories or reliability requirements, the actual grid shape can be adjusted as needed, e.g., triangular or hexagonal grids. It is worth mentioning that, the grid arrangement of gateways, which although seems lack of flexibility, is actually very common in practice [10]. Furthermore, the analytical results based on a grid structure can be used to bound performance of random placement of gateways [11]. For clarity, mathematical notations used in this paper are summarized in Table I.

III. Theoretical Analyses

Considering the *memory-less* characteristic of each retransmission, the probability P_n that a packet is successfully received by the network server, when the tagged end device is in the range of n gateways simultaneously, can be written as

$$P_n = P_{\mathsf{1st}} \cdot P_n^{\mathsf{1st}} + (1 - P_{\mathsf{1st}}) \cdot P_n^{\mathsf{Re}} \quad , \tag{1}$$

where P_{1st} is the probability that the observed transmission is the first attempt of the packet, P_n^{1st} is the probability that the first transmission attempt is successful, and P_n^{Re} is the probability that the packet is successfully received after one or more re-transmissions. These probabilities will be derived in the following parts of this section, respectively.

A. Calculation of P_n^{1st}

According to the condition of packet collision described in the system model, the first attempt for a transmission originated from an end device in the range of n gateways is successful with probability

$$\begin{aligned} P_n^{\mathsf{1st}} &= \sum\nolimits_{m=0}^{M} P_m^{\mathsf{R}} \cdot P_{m,n}^{\mathsf{DATA}} \cdot P_m^{\mathsf{ACK}} \\ &= \sum\nolimits_{m=0}^{M} P_m^{\mathsf{R}} \cdot P_{m,n}^{\mathsf{D-D}} \cdot P_{m,n}^{\mathsf{D-A}} \cdot P_m^{\mathsf{ACK}} \quad , \end{aligned} \tag{2}$$

where $P_{m,n}^{\mathsf{DATA}}$ is the probability that the data packet is transmitted without collision at data rate R_m in the n gateway scenario. $P_{m,n}^{\mathsf{DATA}}$ is the product of two terms: $P_{m,n}^{\mathsf{D-D}}$ and $P_{m,n}^{\mathsf{D-A}}$, which are the probabilities that the observed data packet does not intersect with the transmission of any another data packets, and an ACK packet from a gateway as a response to its previous reception, respectively. Moreover, according to the LoRaWAN specification, ACK transmissions are coordinated by the network server. Hence, even multiple gateways receives the data packet successfully, only one of the gateways will send out the ACK. Therefore, the probability P_m^{ACK} that the expected ACK packet is received in one of the two reception windows, is not directly related to n.

To calculate $P_{m,n}^{\mathsf{D-D}}$, we can define S_i, $i \in [1, n]$, as the event that the desired uplink transmission does not collide with any other data transmissions in gateway G_i's interference region I_i, which is a disk centered at G_i with radius r. With the Inclusion-Exclusion Principle (IEP), $P_{m,n}^{\mathsf{D-D}}$ can be expressed as

$$\begin{aligned} P_{m,n}^{\mathsf{D-D}} &= \Pr\left\{\bigcup\nolimits_{i=1}^{n} S_i\right\} \\ &= \sum\nolimits_{i=1}^{n} \Pr\{S_i\} - \sum\nolimits_{i<j} \Pr\{S_i \cap S_j\} \\ &\quad + \sum\nolimits_{i<j<k} \Pr\{S_i \cap S_j \cap S_k\} - \cdots \\ &\quad + (-1)^{n-1} \Pr\{\cap_{i=1}^{n} S_i\} \quad . \end{aligned} \tag{3}$$

Given the the random selection of the transmitting channel, the equivalent traffic density λ' for the selected channel and data rate R_m can be obtained as $\lambda' = \frac{P_m^{\mathsf{R}}}{C}\lambda$. Moreover, if the observed data transmission starts from time zero, no other data transmissions should be initialized within time duration $[-T_m^{\mathsf{D}}, T_m^{\mathsf{D}}]$, where $T_m^{\mathsf{D}} = L_{\mathsf{D}}/R_m$. Therefore,

$$\Pr\{S_i\} = \left(e^{-2\lambda' T_m^{\mathsf{D}}}\right)^{\rho\mathcal{A}(I_i)-1} = e^{-2\lambda' T_m^{\mathsf{D}}(\rho\mathcal{A}(I_i)-1)} \quad , \tag{4}$$

$$\Pr\{S_i \cap S_j\} = e^{-2\lambda' T_m^{\mathsf{D}}(\rho\mathcal{A}(I_i \cup I_j)-1)} \quad , \tag{5}$$

and generally,

$$\Pr\{\cap_{i=1}^{k} S_i\} = e^{-2\lambda' T_m^{\mathsf{D}}\left(\rho\mathcal{A}\left(\cup_{i=1}^{k} I_i\right)-1\right)} \quad , \quad k \in [1, n] \quad , \tag{6}$$

where $\mathcal{A}(\mathsf{x})$ represents the area of region x. It is clear that, due to the homogeneity of the gateways, $\mathcal{A}(I_i) = \pi r^2$, $i \in [1, n]$. However, the area for the intersection of multiple interference regions depends on the placement of the gateways, which will be derived in Section IV.

If a gateway starts to receive a new data packet, the pending ACK transmission on the same channel is canceled and will be scheduled on a downlink channel later. Therefore, a collision between a data packet and an ACK packet only happens when the ACK is generated within the time interval $[-T_m^{\mathsf{A}}, 0]$, where $T_m^{\mathsf{A}} = L_{\mathsf{A}}/R_m$, and L_{A} is the size of the ACK packet. Since the ACK transmission is initialized only after a data packet is successfully received, the equivalent traffic density of ACK frames in the main channel is $\lambda'' = P_{m,n}^{\mathsf{DATA}} \cdot \lambda'$. Therefor, we have

$$P_{m,n}^{\mathsf{D-A}} = e^{-T_m^{\mathsf{A}}\lambda''} \quad . \tag{7}$$

As mentioned in the system model, once any gateway successfully receives the data packet, the network server will select a gateway to send the first ACK in the first reception window with the same main channel and data rate R_m. If the first ACK transmission is unsuccessful, the second ACK will be sent in the second reception window in the downlink channel and at the lowest data rate R_0. Therefore, P_m^{ACK} can calculated as

$$P_m^{\mathsf{ACK}} = P_m^{\mathsf{ACK\text{-}1}} + P_0^{\mathsf{ACK\text{-}2}} \cdot \left(1 - P_m^{\mathsf{ACK\text{-}1}}\right) \quad , \tag{8}$$

where $P_m^{\mathsf{ACK\text{-}1}}$ and $P_0^{\mathsf{ACK\text{-}2}}$ are the successful probabilities of the first and second ACK transmissions, respectively. By similar arguments, the first ACK is successfully transmitted if no data packet transmission intersects it. Therefore,

$$P_m^{\mathsf{ACK\text{-}1}} = e^{-\left(\min(T_1, T_m^{\mathsf{D}}) + T_m^{\mathsf{A}}\right)\lambda'(\rho\pi r^2)} \quad . \tag{9}$$

The minimum of T_1 and T_m^{D} is taken in (9), because a frame that exceeds T_1 would have collided with the data frame, and thus violates the condition that the data frame was successfully received [1]. The second ACK is received successfully, when data packet transmission is successful but the first ACK fails. This implies that no other ACKs are generated in the downlink channel, namely,

$$P_0^{\mathsf{ACK\text{-}2}} = e^{-2T_0^{A} \cdot (\lambda - \lambda') \cdot \sum_{m=0}^{M} P_{m,n}^{\mathsf{DATA}} P_m^{\mathsf{R}}} \quad . \tag{10}$$

Combining (6)–(10), P_n^{1st} can be derived.

B. Calculation of P_n^{Re}

When the tagged end device cannot receive any ACK before the waiting time exceeds $T_{\mathsf{A\text{-}Out}}$, a retransmission will be initialized after a backoff time interval. The transmission channel will be randomly selected again, while the data rate may change. Due to the space limit, the simplest case, in which the data rate remains the same, is considered here. For a previously collided end device pair, the collision will happen again if the identical transmission channel is selected by both end devices at probability $1/C$, and their transmission durations overlap with each other (Fig. 2). As depicted in the figure, the data transmission starts from time zero and ends at T_m^{D}, while an interfering transmission starts at t_{o}, $t_{\mathsf{o}} \in (0, T_m^{\mathsf{D}})$. The collision is confirmed at $\tau = T_m^{\mathsf{D}} + T_{\mathsf{A\text{-}Out}}$, after which two retransmissions start at t_{R} and t'_{R}, respectively. Based on the random backoff mechanism in LoRaWAN, t_{Re} is uniformly

[1] Note it is possible that an ACK may also collide with a data packet that exceeds T_1 from an end device located within the interference region of the tagged transmitter but not in the interference region of the observed n gateway. For simplicity, here we assume that the union of the n gateway's interference region fully covers the tagged transmitter's interference region. Hence (9) still holds.

distributed in $[\tau, \tau + W]$, and t'_{R} is uniformly distributed in $[\tau + t_{\mathsf{o}}, \tau + t_{\mathsf{o}} + W]$. Therefore, the probability $P_{m,n}^{\mathsf{DATA\text{-}Re}}$ that the data packet is re-transmitted without collision at data rate R_m can be obtained as

$$P_{m,n}^{\mathsf{D\text{-}Re}} = 1 - \frac{2}{C} \frac{\int_0^{T_m^{\mathsf{D}}} \lambda' e^{-\lambda' t_{\mathsf{o}}} \int_0^W \int_{t_{\mathsf{o}}}^{W+t_{\mathsf{o}}} \mathcal{G}(t_{\mathsf{R}}, t'_{\mathsf{R}}) \mathrm{d}t_{\mathsf{R}} \mathrm{d}t'_{\mathsf{R}} \mathrm{d}t_{\mathsf{o}}}{\int_0^{T_m^{\mathsf{D}}} \lambda' e^{-\lambda' t_{\mathsf{o}}} \mathrm{d}t_{\mathsf{o}}} , \tag{11}$$

where

$$\mathcal{G}(t_{\mathsf{R}}, t'_{\mathsf{R}}) = \frac{\mathbf{1}(t_{\mathsf{R}} \le t'_{\mathsf{R}} \le t_{\mathsf{R}} + T_m^{\mathsf{D}}) + \mathbf{1}(t'_{\mathsf{R}} \le t_{\mathsf{R}} \le t_{\mathsf{R}} + T_m^{\mathsf{D}})}{W^2} , \tag{12}$$

and $\mathbf{1}(\cdot)$ is the indicator function. Moreover, P_n^{Re} can be obtained by following (2), while the $P_{m,n}^{\mathsf{DATA}}$ should be replaced with $P_{m,n}^{\mathsf{D\text{-}Re}}$ derived above.

C. Calculation of P_{1st}

Intuitively, the probability P_{1st} for a transmission to be the first attempt after the data packet is generated should be the reciprocal of the average number of transmission attempts for a data packet. Accordingly,

$$P_n^{\mathsf{1st}} = \frac{1}{1 + (1 - P_n^{\mathsf{1st}}) \cdot \sum_{l=0}^{N-1} l (1 - P_n^{\mathsf{Re}})^l P_n^{\mathsf{Re}} P_{\mathsf{N}}^{l+1}} , \tag{13}$$

and

$$P_{\mathsf{N}} = \sum_{m=0}^{M} P_m^{\mathsf{R}} e^{-\lambda' \left(T_m^{\mathsf{D}} (1+T_1) + T_0^{\mathsf{A}} + (1+W/2) \right)} \tag{14}$$

where P_{N} is the probability that no other new data packet is generated by the tagged end device during the time interval of a successful reception, $1 + W/2$ is the average time duration an end device waits before its retransmission.

Combining the formulas (1)–(14), we can obtain the average successful transmission probability P_n for the n gateway coverage scenario.

IV. Related Area Calculations

Recall in (6), to derive the probability of $P_{m,n}^{\mathsf{D\text{-}D}}$, we need to find out the union of the inference regions of a subset of gateways. In this section, the area of the union of two or three gateway interference regions will be derived first. After that, the more general result for the union of any number of gateway interference regions will be obtained.

A. Union Area of Two Gateway Interference Regions

Given two interference regions I_i and I_j, $i, j \in [1, n]$, $\mathcal{A}(I_i \cup I_j)$ can be calculated according to IEP as

$$\mathcal{A}(I_i \cup I_j) = 2\pi r^2 - \mathcal{A}(I_i \cap I_j) = 2\pi r^2 - \mathcal{O}(d_{ij}, r) , \tag{15}$$

where $\mathcal{O}(d_{ij}, r)$ represents the overlapping area between two disks with identical radius r and inter-center distance d_{ij}. As illustrated in Fig. 3, , in the grid placement, the values that d_{ij} can take is discrete. Consider a Cartesian coordinate system with its origin located at the center of the gateway grid, and place G_1 on the positive x axis, the distance $\overline{oG_1}$ is easily derived as

$$\overline{oG_1} = d_{\mathsf{G}} / (2 \sin \tfrac{\alpha}{2}) = \overline{oG_i} , \quad \alpha = 2\pi/n , \quad i \in [1, n] . \tag{16}$$

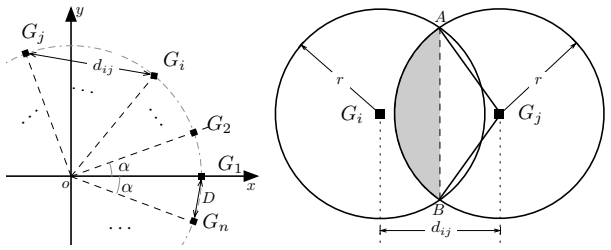

Fig. 3. Illustration for calculating $\mathcal{O}(d_{ij}, r)$

Hence, the distance between G_i and G_j is

$$d_{ij} = \frac{\sin(2\pi(j-i)/n)}{\sin(\pi/n)} \cdot d_{\mathsf{G}} . \tag{17}$$

With d_{ij} and r, the overlapping area of G_i and G_j can be computed as twice the shaded region area in Fig. 3. From the Appendix of [12], we have

$$\mathcal{O}(d_{ij}, r) = 2r^2 \arccos\left(\tfrac{d_{ij}}{2r}\right) - \tfrac{d_{ij}}{4} \sqrt{4r^2 - d_{ij}^2} . \tag{18}$$

B. Union Area of Three Gateway Interference Regions

From IEP, the union area of any three interference regions can be calculated as

$$\begin{aligned} \mathcal{A}(I_i \cup I_j \cup I_k) =& 3\mathcal{A}(I_i) - \sum\nolimits_{\substack{a,b \in \{i,j,k\} \\ a<b}} \mathcal{O}(d_{ab}, r) \\ &+ \mathcal{O}'(d_{ij}, d_{jk}, d_{ik}, r) , \end{aligned} \tag{19}$$

where $\mathcal{O}'(d_{ij}, d_{jk}, d_{ik}, r)$ is the jointly overlapped area of I_i, I_j, and I_k. To calculate $\mathcal{O}'(d_{ij}, d_{jk}, d_{ik}, r)$ for arbitrary $i, j, k \in [1, n]$, a Cartesian coordinate system can be established as depicted in Fig. 4. In the figure, (x_{ij}, y_{ij}), (x_{jk}, y_{jk}), and (x_{ik}, y_{ik}) are the coordinates for the intersection points of G_i, G_j, and G_k's interference region boundaries.

Firstly, due to symmetry, the coordinates (x_{ij}, y_{ij}) can be easily obtained as[2]

$$x_{ij} = d_{ij}/2, \quad y_{ij} = \sqrt{4r^2 - d_{ij}^2}/2 . \tag{20}$$

Normally, calculating (x_{ik}, y_{ik}) requires solving of two equations. However, inspired by [13], utilizing a transformed new coordinate system (x', y'), which is also illustrated in Fig. 4 by counterclockwise rotating the original one with angle θ', allows us to directly express the intersection point's new coordinates as

$$x'_{ik} = d_{ik}/2, \quad y'_{ik} = \sqrt{4r^2 - d_{ik}^2}/2 . \tag{21}$$

Using a proper rotation matrix, we can obtain its coordinates in the original coordinate system,

$$x_{ik} = x'_{ik} \cdot \cos\theta' - y'_{ik} \cdot \sin\theta' \quad \text{and,} \tag{22}$$

$$y_{ik} = x'_{ik} \cdot \sin\theta' + y'_{ik} \cdot \cos\theta' , \tag{23}$$

where θ' can be derived based on the Law of Cosine,

$$\cos\theta' = \frac{d_{ij}^2 + d_{ik}^2 - d_{jk}^2}{2 d_{ij} d_{ik}} . \tag{24}$$

[2]It is worth to mention that, there is actually another intersection point with coordinate $(x_{ij}, -y_{ij})$, but only the meaningful one is used here.

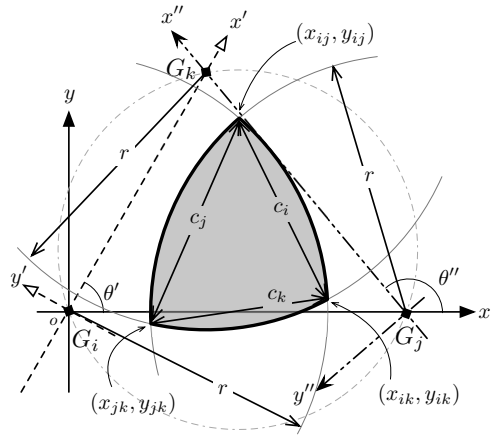

Fig. 4. Illustration for calculating $\mathcal{O}'(d_{ij}, d_{ik}, d_{jk}, r)$

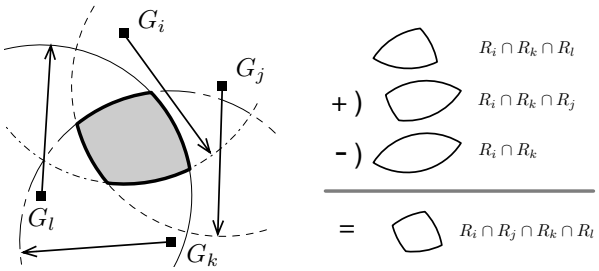

Fig. 5. An example for the intersected area of multiple disks

Similarly, by further rotating the original coordinate system to (x'', y'') depicted in Fig. 4, we have

$$x''_{jk} = d_{jk}/2, \quad y''_{jk} = \sqrt{4r^2 - d_{jk}^2}/2 \quad . \tag{25}$$

Therefore,

$$x_{jk} = x''_{jk} \cdot \cos\theta'' - y''_{jk} \cdot \sin\theta'' + d_{jk} \quad , \tag{26}$$

$$y_{jk} = x''_{jk} \cdot \sin\theta'' + y''_{jk} \cdot \cos\theta'' \quad , \tag{27}$$

$$\cos\theta'' = -\frac{d_{ij}^2 + d_{jk}^2 - d_{ik}^2}{2 d_{ij} d_{jk}} \tag{28}$$

With the coordinates of all three intersection points, the chord length c_x ($l \in \{i, j, k\}$) in the figure can be calculated, and then the area of the intersected circular triangle can be calculated using the result in [13]

$$\begin{aligned} &\mathcal{O}'(d_{ij}, d_{ik}, d_{jk}, r) \\ =&\sqrt{K \prod_x (K - c_x)} + \sum_x r^2 \arcsin\frac{c_x}{2r} - \sum_x \frac{c_x}{4}\sqrt{4r^2 - c_x^2} \end{aligned} \tag{29}$$

where $x \in \{i, j, k\}$, $K = (c_i + c_j + c_k)/2$. Hence, the area $\mathcal{A}(I_i \cup I_j \cup I_k)$ can be obtained from (18), (19), and (29).

C. Union Area of the Interference Regions of Arbitrary l Gateways

Clearly, the calculation of $\mathcal{A}(I_i \cup I_j \cup \cdots \cup S_l)$ relies on the intersection area of several gateways' interference regions or $\mathcal{A}(\cap_{i \in \mathbf{G}} I_i)$, $\mathbf{G} \subseteq \{1, 2, \cdots, n\}$. It is rather laborious to do so for each subset of gateways. Fortunately, Kratky proved in [14] the following result,

Theorem 1 [14]. *The intersection of n disks can always be reduced to contributions from intersections of less than four disks.*

In other words, $\mathcal{A}(\cap_{i \in \mathbf{G}} I_i)$ can be calculated with previously obtained results, i.e., $\mathcal{A}\{I_i \cup I_j\}$ and $\mathcal{A}\{I_i \cup I_j \cup I_k\}$. An intuitive example for computing the intersection of four disks is given in Fig. 5. Formally, a general method to calculate the intersecting area of any number of interference regions, is given by the following lemma.

Lemma 1. *For a given set of gateways $\mathbf{G}$, $\mathbf{G} \subseteq \{1, 2, \cdots, n\}$, by arbitrarily picking two gateways G_i and G_j, $i, j \in [1, n]$, $d_{ij} > d_{\mathsf{G}}$, the intersected area for the interference region of gateways in $\mathbf{S}$ can be decomposed to*

$$\mathcal{A}\Big(\bigcap_{l \in \mathbf{S}} I_l\Big) = \mathcal{A}\Big(\bigcap_{\substack{l \in \mathbf{S} \\ l \neq i}} I_l\Big) + \mathcal{A}\Big(\bigcap_{\substack{l \in \mathbf{S} \\ l \neq j}} I_l\Big) - \mathcal{A}\Big(\bigcap_{\substack{l \in \mathbf{S} \\ l \neq i,j}} I_l\Big) \quad .$$

When $|\mathbf{G}| - 1 > 3$, the above equation can be applied iteratively, until the overlapped area corresponds to that of two or three intersecting disks.

V. Performance Evaluation

To verify the analytical model, we conduct several numerical simulations. Following the LoRaWAN specification, we consider a network operating on the EU 863-880 MHz ISM band with channel bandwidth 125 kHz. The probability for choosing different data rates are distributed as: $P_0^{\mathsf{R}} = 0.28$, $P_1^{\mathsf{R}} = 0.20$, $P_2^{\mathsf{R}} = 0.14$, $P_3^{\mathsf{R}} = 0.10$, $P_4^{\mathsf{R}} = 0.08$, $P_5^{\mathsf{R}} = 0.20$. The transmission range and interference range are set to 800 m and 1 km. In the simulations and analysis, we vary the IoT device density from 80 nodes/km^2 (approximately 250 nodes per interference region) to 480 nodes/km^2 (approximately 1500 nodes per interference region). Each data packet is assumed to have the maximum 51 bytes payload length, and the traffic generation intensity varies from 0.15 packets/s to 0.90 packets/s.

The simulation results are summarized in Fig. 6 – Fig. 8. As can be seen from Fig. 6, increasing the number of gateways that concurrently covers an end device can significantly improves its transmission reliability. However, the gain is reduced as more gateways are introduced. This is because that, given a fixed transmission power, the size of the area that contains all potential interferers to the tagged end device actually is upper bounded by $\pi(2r)^2$. Therefore, the benefit of more gateways is reduced for a large n. From Fig. 7, we see that the successful transmission probabilities for both first attempt and after retransmissions decreased significantly when the traffic intensity is increased. . This is intuitive as there are more collisions as the traffic intensity grows. Interestingly, the negative impact of higher traffic intensity is more profound on the retransmissions than the first transmission attempts. This is mainly because a fixed back off window is insufficient to randomize the retransmission of previously collided packets. This suggests for high density LoRaWAN, schemes such as

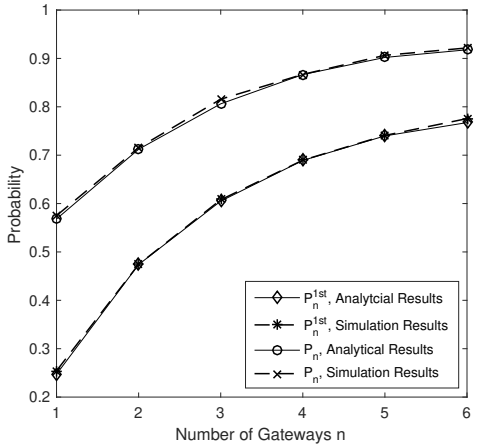

Fig. 6. First Attempt Successful Probability P_n^{1st} and ASTP P_n, λ = 0.60 packets / second, ρ = 320 nodes / km^2

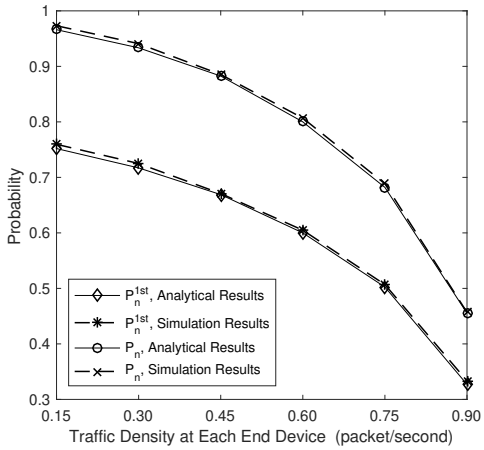

Fig. 7. First Attempt Successful Probability P_n^{1st} and ASTP P_n, ρ = 320 nodes / km^2, n = 3

exponential random backoff are more suitable. Figure 8 shows as the device density grows, both probabilities drop. One potential application of the analytic model in this work is to provision LoRaWAN with suitable number of gateways and maximally allowed device density given Quality of Service requirements.

VI. Conclusions

In this paper, the impact of redundant packet reception at gateways on data reliability was studied for LoRaWANs under the protocol interference model. The Average Successful Transmission Probability (ASTP) was represented as a function of the end device density, gateway density, and traffic intensity. As future work, we plan to conduct further analysis using a more realistic physical interference model, which takes into account the signal-to-interference ratio at receiver in determining whether a transmission is successful.

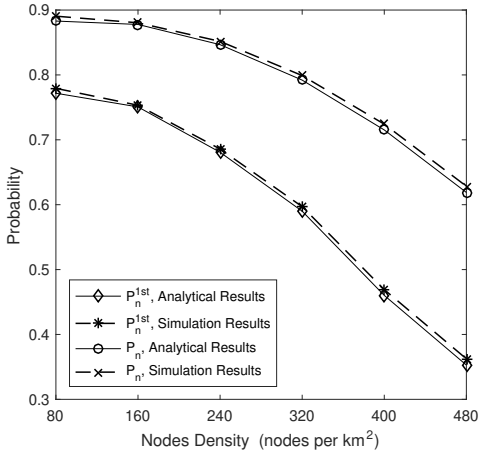

Fig. 8. First Attempt Successful Probability P_n^{1st} and ASTP P_n, λ = 0.60 packets / second, n = 3

Moreover, we also plan to relax the grid placement constraint on gateways, which will lead to more generic results.

References

[1] "LoRa Alliance Wide Area Networks for IoT," *LoRa Allinace [Online]. Available: https://www. lora-alliance. org/*, 2016.

[2] T. Wendt, F. Volk, and E. Mackensen, "A benchmark survey of long range (LoRa) spread-spectrum-communication at 2.45 ghz for safety applications," in *Proc. of Wireless and Microwave Technology Conference (WAMICON)*, 2015, pp. 1–4.

[3] E. D. Ayele, C. Hakkenberg, J. P. Meijers, K. Zhang, N. Meratnia, and P. J. Havinga, "Performance analysis of LoRa radio for an indoor IoT applications," in *Proc. of Internet of Things for the Global Community (IoTGC)*, 2017.

[4] J. Petäjäjärvi, K. Mikhaylov, M. Pettissalo, J. Janhunen, and J. Iinatti, "Performance of a low-power wide-area network based on LoRa technology: Doppler robustness, scalability, and coverage," *International Journal of Distributed Sensor Networks*, vol. 13, no. 3, p. 1550147717699412, 2017.

[5] K.-H. Phung, H. Tran, Q. Nguyen, T. T. Huong, and T.-L. Nguyen, "Analysis and assessment of LoRaWAN," in *Proc. of Recent Advances in Signal Processing, Telecommunications & Computing (SigTelCom)*, 2018, pp. 241–246.

[6] M. Rizzi, P. Ferrari, A. Flammini, and E. Sisinni, "Evaluation of the IoT LoRaWAN solution for distributed measurement applications," *IEEE Transactions on Instrumentation and Measurement*, vol. 66, no. 12, pp. 3340–3349, 2017.

[7] K. Mikhaylov, J. Petaejaejaervi, and T. Haenninen, "Analysis of capacity and scalability of the LoRa low power wide area network technology," in *Proc. of European Wireless*, 2016, pp. 1–6.

[8] O. Georgiou and U. Raza, "Low power wide area network analysis: Can LoRa scale?" *IEEE Wireless Communications Letters*, vol. 6, no. 2, pp. 162–165, 2017.

[9] P. Gupta and P. R. Kumar, "The capacity of wireless networks," *IEEE Trans. Inf. Theory*, vol. 46, no. 2, pp. 388–404, Mar. 2000.

[10] H. Farman, H. Javed, J. Ahmad, B. Jan, and M. Zeeshan, "Grid-based hybrid network deployment approach for energy efficient wireless sensor networks," *Journal of Sensors*, vol. 2016, Article ID 2326917, 2016.

[11] F. Xue and P. R. Kumar, "Scaling laws for ad hoc wireless networks: An information theoretic approach," *Foundations and Trends® in Networking*, vol. 1, no. 2, pp. 145–270, 2006.

[12] M. Ni, L. Zheng, F. Tong, J. Pan, and L. Cai, "A Geometrical-Based throughput bound analysis for Device-to-Device communications in cellular networks," *IEEE J. Sel. Areas Commun.*, vol. 33, no. 1, pp. 100–110, Jan. 2015.

[13] M. P. Fewell, "Area of common overlap of three circles," Defence Science and Technology Organisation Edinburgh (Australia) Maritime Operations Div., Tech. Rep., 2006.

[14] K. W. Kratky, "The area of intersection of n equal circular disks," *J. Phys. A Math. Gen.*, vol. 11, no. 6, p. 1017, Jan. 2001.